

Thermal transition measurements of polymer thin films by modulated nanoindentation

Scott Sills

Department of Chemical Engineering, University of Washington, Seattle, Washington 98195

Hanson Fong

Department of Materials Science and Engineering, University of Washington, Seattle, Washington 98195

Cynthia Buenviaje

Department of Chemical Engineering, University of Washington, Seattle, Washington 98195

Mehmet Sarikaya

Department of Materials Science and Engineering, University of Washington, Seattle, Washington 98195

René M. Overney^{a)}

Department of Chemical Engineering, University of Washington, Seattle, Washington 98195

(Received 17 February 2005; accepted 6 May 2005; published online 1 July 2005)

A modulated nanoindentation technique has been developed for thermal transition analysis of polymer thin films. The procedure was applied to glass transition measurements of poly-*t*-butylacrylate, with results that compare well with shear-modulated force microscopy and differential scanning calorimetry. The advantages of the modulated indentation technique are twofold: (i) it provides *in situ* experimental access to material properties in nanoscopically confined geometries, and (ii) it incorporates well-defined indenter geometries, which provide a means for quantitative thermorheological analysis that is not available with conventional scanning probe microscopy. The experimental procedure and critical test parameters are detailed. © 2005 American Institute of Physics. [DOI: 10.1063/1.1943508]

I. INTRODUCTION

The technological drive for introducing nanoscopic devices is faced with the breakdown of continuum theories and traditional scaling approaches. In this mesoscopic regime, material and transport properties become dominated by interfacial and dimensional constraints. Hence, macroscopic characterization efforts often fail to accurately describe material behaviors in confined geometries.¹ In this light, there is a pressing need for highly localized techniques, capable of probing molecular behaviors *in situ*, in confined geometries. Specifically, material property measurements at the submicron level are essential for the characterization of miniaturized electronic, optical, mechanical, and biomedical devices.^{2,3}

Progress in this direction strongly depends on the development of appropriate techniques used to analyze surface and rheological properties on the micro- and nanometer scales. Over the past two decades, several contact mechanical approaches have been developed to meet these needs; e.g., the surface forces apparatus (SFA),⁴ the scanning force microscope (SFM),⁵ and depth-sensing nanoindentation.⁶ Interest in these techniques has been motivated by the attainable high spatial and force resolutions. Numerous variations of these methods have evolved for quantitative measurements on the nanometer scale. Specifically, force modulation

techniques⁷ have offered significant improvement to the sensitivity of traditional SFM and nanoindentation approaches.^{2,3,8,9}

Contact mechanical characterization efforts using modulated probing techniques seek to infer material specific information from the elastic (or dissipative) nature of the probing contact. For example, thermally induced transition properties, such as the glass transition, could be measured by shear-modulated force microscopy (SM-FM) in thin films.⁸ SM-FM has proved to be particularly useful in single asperity friction analyses,¹⁰ and in determining cross-linking densities³ and structural phase transitions⁹ of ultrathin films. One limitation of the SFM is that no satisfactory quantitative method exists for contact mechanical analysis because of poorly defined tip geometries. With nanoindentation, tip characterization methods are available,¹¹ allowing the contact area to be defined and permitting an adequate quantitative analysis.

Building on the success of force-modulated SFM and the quantitative benefits of nanoindentation, this work introduces a modulated nanoindentation procedure for measuring thermal transitions on polymer films. The experimental procedure and the effects of critical test parameters are highlighted. The technique is employed to measure the glass transition temperature (T_g) of polymer thin films, and the results are compared to T_g values obtained by SM-FM and differential scanning calorimetry (DSC).

II. EXPERIMENT

The modulated indentation analysis involves a commercial SFM (Veeco, Discoverer) in conjunction with a nanoin-

^{a)}Author to whom correspondence should be addressed; electronic mail: roverney@u.washington.edu

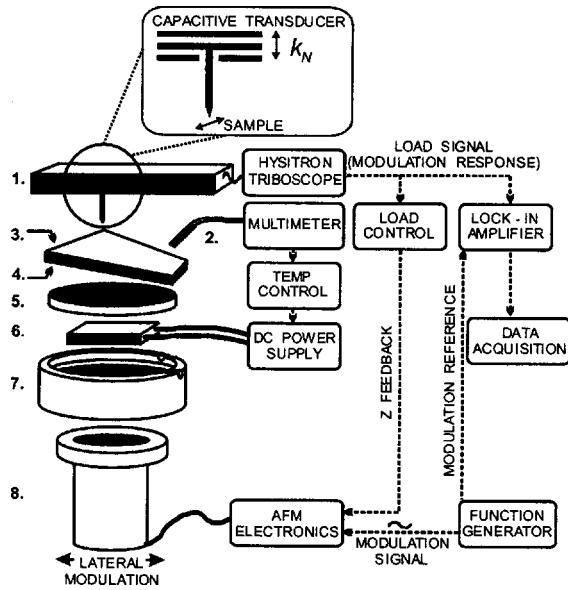


FIG. 1. Physical and electronic configurations of the shear-modulated nanoindentation technique used for measuring thermal transitions of polymer films. (1) Hysitron Triboscope (capacitive load-displacement transducer). (2) Thin-film detector temperature sensor. (3) Polymer film sample. (4) Sample substrate (silicon). (5) Copper disk. (6) Thermoelectric heater. (7) Macor heater housing. (8) Piezoelectric tube scanner of a Topometrix Discoverer SFM. Outtake: Schematic illustrating the indenter plate in the capacitive transducer (k_N =indenter normal spring constant).

dention system (Hysitron Triboscope, $k_N=149$ N/m). The indenter operates as a single axis, capacitive, load-displacement transducer, which has been discussed elsewhere.² The instrumental setup is pictured in Fig. 1. Samples are typically in the form of substrate-supported thin polymer films, which are glued to a copper disk on top of the heater stage assembly, items 3, 4, and 5 in Fig. 1. A noncompliant, high-conductivity thermal compound is applied between the substrate and copper disk to promote uniform heating. No significant difference in the load frame compliance is observed between glued or mechanically clamped samples.

Temperature control is provided with a small thermo-electric heater (Ferrotec America Corp.), which is fixed in a machined Macor housing, items 6 and 7 in Fig. 1, respectively. The heater is powered with a dc power supply (HP 6653A), and the heater stage is anchored to the magnetic head of the SFM scanner, item 8 in Fig. 1, with a steel disk in the bottom of the Macor housing (not illustrated). A resistive temperature sensor (thin-film detector, Omega Inc.) is fixed to the sample surface with thermal compound and glue, item 2 in Fig. 1. All temperature measurements are recorded directly at the polymer film surface. The sample temperature is monitored with a multimeter (HP 34401A) and controlled within ± 0.1 °C using a standard proportional, integral, differential (PID) feedback loop in LABVIEW (National Instruments).

Measurements are conducted with the indenter in contact with the sample, under a constant applied load of 1–5 μ N. Note, there is no prescribed loading schedule for the thermal transition measurements discussed here. Instead, a nanoscopic shear perturbation is applied to the sample, through the x channel of the piezoelectric tube scanner of the SFM.

The modulation signal is provided in the form of a sine wave, with a function generator (SRS D5345). The frequency is selected from a frequency spectrum of the operating system, avoiding any system resonances and ranging from 0.5 to 1 kHz. The modulation amplitude is chosen small enough to avoid any relative tip-sample sliding, and ranges from 5 to 9 nm.

A lateral versus normal perturbation is preferred in order to maintain a constant load. However, the single axis Hysitron nanoindenter is primarily sensitive to normal displacements, i.e., $k_T \gg k_N$, and a small sample tilt ($<5^\circ$) is necessary to create a subnanometer normal component of the lateral modulation. The normal force component of the modulation (<60 nN) was small compared to the applied normal load (1–5 μ N), and the modulation frequency was higher than that of the load control feedback loop, i.e., the feedback was unaware of the small, fast normal modulation component acting on the tip. Thus, in principle, a small amplitude, normal modulation technique, should provide similar results, provided that the load changes associated with the modulation displacement are small with respect to the equilibrium load.

The normal forces acting on the tip are imposed on the load-displacement transducer signal and are analyzed with respect to the input modulation using a two-channel lock-in amplifier (SRS SR830 DSP). For each temperature step, a thermal equilibration period between 15 and 60 s, depending on the temperature step, ΔT , is allowed before the amplitude and phase response of the transducer signal are recorded and averaged over a 15 s interval.

The amplitude response in no-slip modulated contact experiments is a direct measure of the elastic constant, $k_{\text{tot},z}$, for the system in which the displacements occur.¹² The total normal displacement Δz , is dictated by the normal modulation amplitude, and is distributed between elastic deformation of the contact, Δz_c , and the displacement of the capacitive plate in the indenter transducer, Δz_N . Thus, the sample-indenter system may be modeled as two springs in series, with $\Delta z = \Delta z_c + \Delta z_N$. In this scenario, the experimental observable, $k_{\text{tot},z}$, is related to the sample-tip contact stiffness $k_{c,z}$ and the indenter stiffness k_N , by

$$\frac{1}{k_{\text{tot},z}} = \frac{1}{k_{c,z}} + \frac{1}{k_N}. \quad (1)$$

The indenter stiffness $k_N=149$ N/m, may be considered constant; hence, any changes in the measured elastic constant may be attributed to changes in the contact stiffness $k_{c,z}$. According to the elastic Hertz model, the normal contact stiffness is given by¹²

$$k_{c,z} = 2aE^*, \quad (2)$$

where a is the contact radius, which for a Hertzian hemispherical indenter is $a = [(3RF_N)/(4E^*)]^{-1/3}$ (Ref. 12). Note: Changes in the contact radius due to creep are discussed below. R is the relative curvature of the two contacting materials, i.e., $R = (1/R_1 + 1/R_2)^{-1}$, and E^* is the reduced modulus:

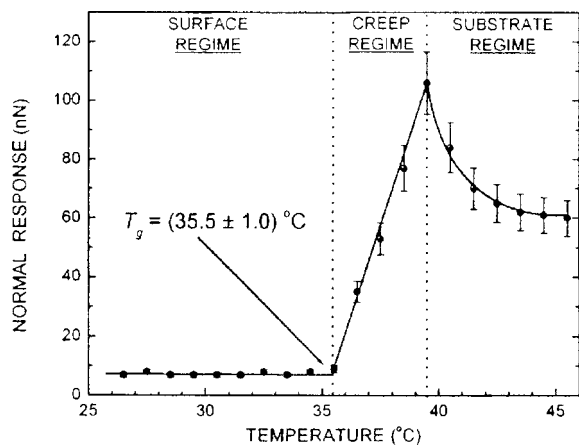


FIG. 2. Modulated nanoindentation T_g results for PtBA with an average heating rate of $0.9\text{ }^\circ\text{C}/\text{min}$. (hemispherical tungsten indenter; $F_N=1.0\text{ }\mu\text{N}$, modulation frequency $=900\text{ Hz}$, and modulation amplitude $=7\text{ nm}$). A T_g value of $35.5\pm 1.0\text{ }^\circ\text{C}$ is indicated by the discontinuous rise in the normal response.

$$E^* = \left(\frac{1 - \nu_1^2}{E_1} + \frac{1 - \nu_2^2}{E_2} \right)^{-1}, \quad (3)$$

with E_1 and E_2 as the elastic moduli of the sample and the probing tip, respectively, and ν_1 and ν_2 are the corresponding Poisson's ratios.¹³

The effect of tip geometry on the resulting amplitude response was assessed with blunt, hemispherical tungsten ($R_2 \sim 1\text{ }\mu\text{m}$) and sharp, diamond Berkovich indenters ($R_2 \sim 50\text{ nm}$). Because the moduli of tungsten and diamond are much greater than those of the compliant polymer samples, i.e., $E_2 \gg E_1$, the reduced modulus in Eq. (3) becomes sensitive primarily to changes in the sample modulus. Thereby, any thermally induced changes in the measured amplitude response reflect a corresponding change in the sample modulus. Generally, a polymer's modulus changes at thermal transition points, for example, by several orders of magnitude at the glass transition. Hence, modulated contact stiffness measurements offer a practical means of tracking thermal transition temperatures.

The procedure was tested with a sample of poly-*t*-butylacrylate ($M_w=137.3\text{ k}$) (PtBA). The sample was spin cast onto a silicon 001 substrate wafer and annealed above its glass transition temperature in a vacuum oven. A film thickness of $172\pm 6\text{ nm}$ was measured by ellipsometry.

III. RESULTS AND DISCUSSION

The thermorheological analysis using the modulated indentation procedure is shown for PtBA in Fig. 2. The amplitude response curve in Fig. 2 resembles the one obtained with SM-FM in Fig. 3(a). Similar to the SM-FM technique,^{9,14} the glass transition temperature is indicated by the first *kink* in the amplitude response in Fig. 2. A T_g value of $35.5\pm 1.0\text{ }^\circ\text{C}$ is determined with the modulated indentation technique, which compares well with the T_g values of $37\pm 2\text{ }^\circ\text{C}$ and $\sim 40\text{ }^\circ\text{C}$ that were obtained for the same material, using SM-FM and DSC, in Figs. 3(a) and 3(b), respectively.

Three distinct regimes are apparent in Fig. 2: The *sur-*

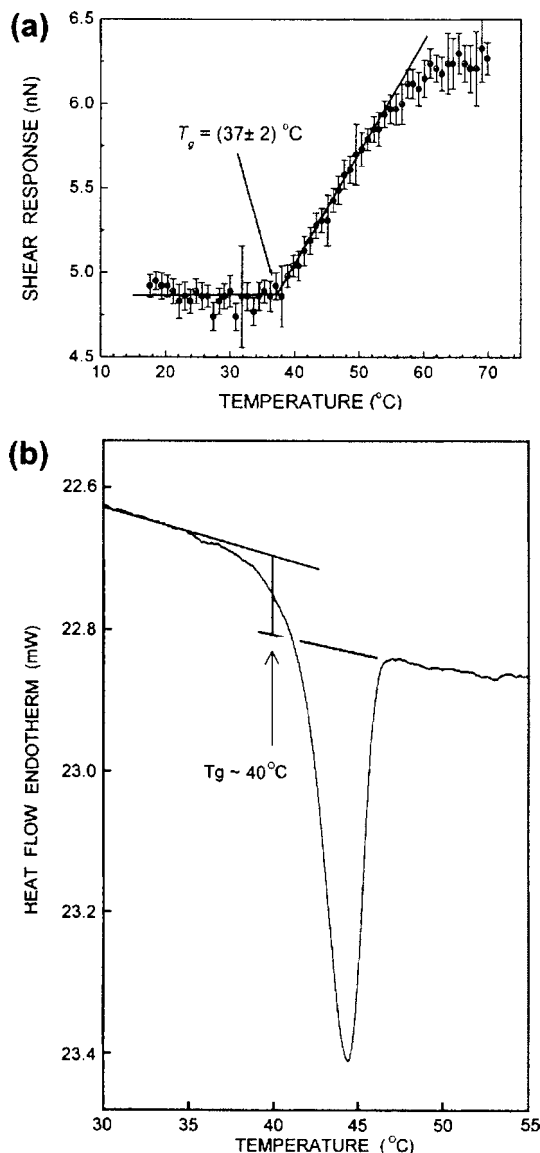


FIG. 3. (a) Shear-modulated force microscopy (SM-FM) results on the same PtBA film indicate a T_g of $37\pm 2\text{ }^\circ\text{C}$ ($F_N=1.0\text{ nN}$, modulation frequency $=4\text{ kHz}$, and modulation amplitude $=14\text{ nm}$). (b) Differential scanning calorimetry (DSC) results for bulk PtBA indicate a T_g of approximately $40\text{ }^\circ\text{C}$.

face regime where $T < T_g$ and the indenter tip remains on the sample surface; the *creep regime* where $T \sim T_g$ and the stylus starts to creep into the polymer; and the *substrate regime* where $T > T_g$ and the indenter tip approaches a dynamic equilibrium with the sample after creeping through the polymer to the substrate. In the surface regime, the normal response of the indenter remains independent of temperature, revealing a constant contact stiffness. Therefore by Eq. (2), it may be concluded that the contact area and sample modulus are constant, and the indenter tip remains on the sample surface without creeping into the polymer.

At $T=T_g$, the creep regime is entered, and the contact stiffness increases with temperature. Considering Eq. (2) and the well-known modulus reduction above T_g , the increased contact stiffness must be accompanied with an increase in the contact radius. Thus, the indenter must penetrate the sample surface and creep into the polymer film. The simplest

material that exhibits steady creep is a Maxwell solid, i.e., a spring and dashpot in series. The creep compliance function for a Maxwell solid is¹³

$$\Phi_1(t) = \left(\frac{1}{E_1} + \frac{1}{\eta_1} t \right), \quad (4)$$

where E and η represent the modulus and viscosity, respectively. For a hemispherical indenter under a constant applied load F_N , the change in the contact radius with time, due to creep, is expressed as¹³

$$a(t)^3 = \frac{3}{8} R F_N \Phi_1(t). \quad (5)$$

Substituting Eqs. (4) and (5) into Eq. (2) gives a contact stiffness of the form

$$k_{c,z} = (3RF_N)^{1/3} (1 - \nu_1^2)^{-1} \left(E_1^2 + \frac{E_1^3}{\eta_1} t \right)^{1/3}. \quad (6)$$

The first term on the right-hand side of Eq. (6) is constant. Under the assumption of incompressibility, the second term may also be considered constant. Generally both the modulus and the viscosity decrease above the glass transition; and thus, the contact stiffness can only increase if $E^3 t / \eta > E^2$. If the viscosity is expressed in terms of the material relaxation time for the Maxwell solid, i.e., $\tau = \eta / E$ (Refs. 13 and 15), the criteria for an increasing contact stiffness in the creep regime become $t / \tau > 1$. Based on an average heating rate of $0.9^\circ\text{C}/\text{min}$, and a creep regime in Fig. 2 that spans 4°C , the experimental *creep time*, t , is 4.4 min. The appropriate material relaxation time for PtBA at $T \geq T_g$ is the α relaxation time, τ_α . Considering that τ_α is typically a subsecond quantity, i.e., $t > \tau_\alpha$, we may conclude that the increase in the contact area due to creep dominates the modulus reduction in their contributions to the contact stiffness in Eq. (2).

After the tip has penetrated the polymer film, the substrate regime is entered. At this point, the rigid substrate prevents further penetration of the indenter and the contact area remains constant. The decreasing contact stiffness with further increased temperature reflects a continued reduction in the sample modulus as tip and sample relax toward a dynamic equilibrium.

The indenter tip geometry was found to affect the shape of the resulting amplitude response curve. With the blunt tungsten indenter, the contact stiffness in Fig. 2 reveals a discrete transition at T_g . We should note that smooth, gradual transitions are observed at higher loads with sharper tips such as a diamond Berkovich indenter. This behavior suggests that the indenter tip penetrates the polymer surface prior to the glass transition, increasing the contact area by means other than creep. For example, the internal pressure of the sample may be insufficient to support the higher contact pressures associated with sharper indenters, thereby giving way to plastic yielding. Consequently, we have found that low equilibrium loads ($\sim 1 \mu\text{N}$) offer a more precise T_g value when using sharp indenters.

Another parameter that contributes to the shape of the measured T_g curve is the sample heating rate. Once T_g has been reached, the slope of the normal response in the creep

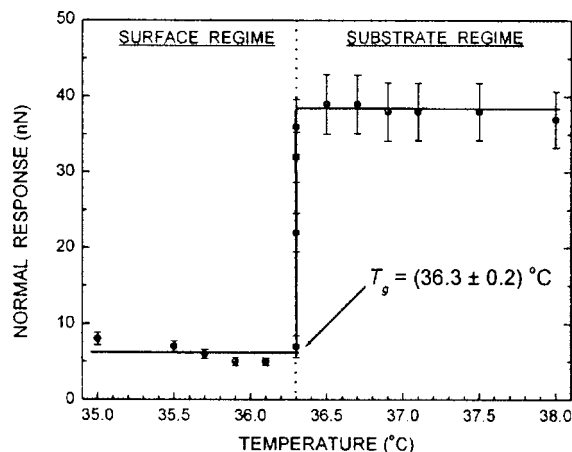


FIG. 4. Modulated nanoindentation T_g results for PtBA, with an average heating of $0.06^\circ\text{C}/\text{min}$ (hemispherical tungsten indenter; $F_N = 1.0 \mu\text{N}$, modulation frequency = 1000 Hz , and modulation amplitude = 9 nm). A T_g value of $36.3 \pm 0.2^\circ\text{C}$ is indicated by the discrete step in the normal response.

regime depends on the heating rate. Note, the measured value of T_g is not affected by the heating rate, only the creep behavior for $T \geq T_g$. For an average heating rate of $0.9^\circ\text{C}/\text{min}$, a positive, noninfinite slope of the amplitude response in the creep regime, as in Fig. 2, indicates that the indenter continues to creep into the polymer, while the temperature continues to increase. This suggests that the heating rate is faster than the creep rate. Conversely, for an average heating rate of $0.06^\circ\text{C}/\text{min}$, the measured amplitude response shows an infinite slope in the creep regime, i.e., the discontinuous jump at T_g from the surface regime directly to the substrate regime in Fig. 4. This suggests that the indenter tip penetrates the polymer film and reaches the substrate prior to an appreciable temperature change, which indicates that the heating rate is slower than the creep rate. It is apparent in Fig. 4 that the accuracy of the measured transition temperature is limited by the precision of temperature controller, not the precision of modulation measurement. While the accuracy of DSC measurements is limited by heat-flow time delays and measurement precision, the modulated technique may become even more attractive by increasing the accuracy of the temperature measurement.

In terms of the heating rate, a more precise T_g measurement is obtained for a slower heating rate at the expense of longer experimental times. Note the difference in the temperature scales in Figs. 2 and 4. Generally, when dealing with a sample of unknown T_g , the best experimental approach has been to first analyze the sample using a heating rate of $\sim 1^\circ\text{C}/\text{min}$ to determine a rough value for T_g . Then, the sample may be retested with a slower heating rate over a more narrow temperature range if a more precise value of T_g is desired.

IV. CONCLUSIONS

A method for analyzing thermal transitions of organic materials has been developed and applied to measure the glass transition temperature, T_g of PtBA thin films. The method stems from the principle of shear-modulated force

microscopy (SM-FM) and employs a nanoscopic sinusoidal perturbation between the sample and a nanoindenter tip. The capacitive load-displacement transducer of the indenter acts as a rheological sensor, which is extremely sensitive to thermally induced changes in the sample modulus, particularly at the glass transition where the modulus drops several orders.

The combined lateral and normal force modulation approach employed in this study was used because of current system limitations, i.e., the single axis nanoindenter is only sensitive to normal perturbations. Therefore, a slight tip-sample angle was used to create a normal component of the lateral modulation. The success of thermal transition measurements with both lateral and normal modulations is a testament to the robustness of rheological techniques that incorporate a contact mechanical analysis with nanoscopic mechanical perturbations.

Both the tip geometry and the heating rate affect the shape of the resulting amplitude response curve. We have found that low equilibrium loads ($\sim 1 \mu\text{N}$) are required when using sharp Berkovich indenters ($R_2 \sim 50 \text{ nm}$). This results from the higher contact stress, relative to blunt tips ($R_2 \sim 1 \mu\text{m}$), where the sharp tip tends to plastically *cut* into the sample, penetrating prior to the onset of the thermal transition. The blunt tips tend to stay on the sample surface prior to the glass transition and can support higher loads. In regard to the heating rate, the slope of the amplitude response immediately following T_g was found to depend on the ratio of the heating rate to the creep rate; however, the transition temperature itself was not affected.

The accuracy of the presented method compares well with established T_g measurement techniques, namely, SM-FM and differential scanning calorimetry (DSC). Compared to DSC, which is best suited for bulk property measurements, one advantage of modulated indentation is its ability to track thermorheological transitions in confined sample geometries. SM-FM also offers this capability; however, characteristic of scanning probe microscopy, SM-FM lacks a satisfactory quantitative contact mechanical analysis because of poorly defined tip geometries. With depth-sensing

indentation, sophisticated methods are available to define the tip geometry, and hence, an absolute quantitative analysis of material properties is possible. Future work seeks to incorporate the modulated technique in determining the thermal dependence of viscoelastic functions, i.e., creep compliance and relaxation modulus, as well as the apparent activation energies for relaxation processes.

ACKNOWLEDGMENTS

The authors wish to thank Oden Warren and Hysitron Inc. for instrumental support and the University of Washington Center for Nanotechnology for funding. Also, we thank Dr. Martin Bammerlin for electronic support, and Dr. Jeffrey Sopp for fabrication of the tungsten tip.

¹R. M. Overney and S. E. Sills, in *Interfacial Properties on the Submicrometer Scale*, edited by J. Frommer and R. M. Overney (American Chemical Society, Washington, DC, 2000), Vol. 781, pp. 2–21.

²S. A. S. Asif, K. J. Wahl, and R. J. Colton, *Rev. Sci. Instrum.* **70**, 2408 (1999).

³R. Luginbuhl, R. M. Overney, and B. D. Ratner, in *Interfacial Properties on the Submicrometer Scale*, edited by J. Frommer and R. M. Overney (American Chemical Society, Washington, DC, 2000), Vol. 781, pp. 178–96.

⁴J. N. Israelachvili and D. Tabor, *Proc. R. Soc. London, Ser. A* **331**, 19 (1972).

⁵G. Binnig, C. F. Quate, and C. Gerber, *Phys. Rev. Lett.* **56**, 930 (1986).

⁶J. B. Pethica, R. Hutchings, and W. C. Oliver, *Philos. Mag. A* **48**, 593 (1983).

⁷J. B. Pethica and W. C. Oliver, *Phys. Scr., T* **T19A**, 61 (1987).

⁸R. M. Overney, E. Meyer, J. Frommer, H. J. Guentherodt, M. Fujihara, H. Takano, and Y. Gotoh, *Langmuir* **10**, 1281 (1994).

⁹R. M. Overney, C. Buenviaje, R. Luginbuhl, and F. Dinelli, *J. Therm. Anal. Calorim.* **59**, 205 (2000).

¹⁰O. Pietrement, J. L. Beaudoin, and M. Troyon, *Tribol. Lett.* **7**, 213 (1999).

¹¹W. C. Oliver and G. M. Pharr, *J. Mater. Res.* **7**, 1564 (1992).

¹²E. Meyer, R. M. Overney, K. Dransfeld, and T. Gyalog, *Nanoscience: Friction and Rheology on the Nanometer Scale* (World Scientific, Singapore, 1998).

¹³K. L. Johnson, *Contact Mechanics* (Cambridge University Press, Cambridge, UK, 1985).

¹⁴S. Sills and R. M. Overney, in *Applied Scanning Probe Methods II*, edited by B. Bushan and H. Fuchs (Springer, Heidelberg, in press).

¹⁵J. D. Ferry (Wiley, New York, 1980), Chap. 11.